

Quasar jet emission model applied to the microquasar GRS 1915+105

M. Türlér^{1,2}, T. J.-L. Courvoisier^{1,2}, S. Chaty^{3,4}, and Y. Fuchs⁴

¹ INTEGRAL Science Data Centre, ch. d'Ecogia 16, 1290 Versoix, Switzerland

² Observatoire de Genève, ch. des Maillettes 51, 1290 Sauverny, Switzerland

³ Université Paris 7, 2 place Jussieu, 75005 Paris, France

⁴ Service d'Astrophysique, DSM/DAPNIA/SAP, CEA/Saclay, 91191 Gif-sur-Yvette, Cedex, France

Received 18 December 2003 / Accepted 14 January 2004

Abstract. The true nature of the radio emitting material observed to be moving relativistically in quasars and microquasars is still unclear. The microquasar community usually interprets them as distinct clouds of plasma, while the extragalactic community prefers a shock wave model. Here we show that the synchrotron variability pattern of the microquasar GRS 1915+105 observed on 15 May 1997 can be reproduced by the standard shock model for extragalactic jets, which describes well the long-term behaviour of the quasar 3C 273. This strengthens the analogy between the two classes of objects and suggests that the physics of relativistic jets is independent of the mass of the black hole. The model parameters we derive for GRS 1915+105 correspond to a rather dissipative jet flow, which is only mildly relativistic with a speed of $0.60c$. We can also estimate that the shock waves form in the jet at a distance of about 1 AU from the black hole.

Key words. radiation mechanisms: non-thermal – stars: individual: GRS 1915+105 – infrared: stars – radio continuum: stars

1. Introduction

Microquasars are high-energy binary systems exhibiting jets with apparent superluminal motion suggesting that they are the miniature replicates in our Galaxy of the distant quasars (Mirabel & Rodríguez 1998). GRS 1915+105 was the first microquasar discovered (Mirabel & Rodríguez 1994) and can be considered as an archetypical object of its class. Its radio emission can be divided into three distinct states: a plateau jet, pre- and post-plateau flares and radio oscillation events (Klein-Wolt et al. 2002). The flares are the most powerful events. Their emission arises from two emitting blobs observed to move relativistically in opposite directions up to about 3000 AU from the core (Fender et al. 1999). This has been interpreted as evidence for pairs of plasma clouds symmetrically ejected on both sides of the accretion disc (Rodríguez & Mirabel 1999). This plasmoid ejection model is also used to explain the less powerful oscillation events arising in a shorter jet extending only up to ~ 30 – 50 AU (Dhawan et al. 2000). This interpretation is supported by the observation of simultaneous X-ray dips, suggesting that material from the disappearing inner accretion disc is ejected from the black hole vicinity (Belloni et al. 1997a,b; Mirabel et al. 1998; Eikenberry et al. 1998).

Observational evidence for this phenomenon has recently also been obtained for the active galaxy 3C 120 (Marscher et al. 2002). This discovery, by strengthening the analogy between galactic and extragalactic objects, rises the question on the true nature of the synchrotron emitting material. Is the microquasar plasmoid model or the quasar shock wave model the correct interpretation? Atoyan & Aharonian (1999) showed that expanding clouds of relativistic plasma cannot describe the observations unless there is an in situ electron acceleration process. An alternative model of a variable continuous jet also fails to explain the observed flux oscillations in GRS 1915+105 as it leads to unphysically large electron densities (Collins et al. 2003). There is therefore growing evidence that the emitting electrons must be reaccelerated along the jet, as it is the case in a shock wave mechanism (Kaiser et al. 2000).

To further test the shock wave interpretation, we apply here to GRS 1915+105 the same model used to describe the long-term variability behaviour of 3C 273 from submillimeter to radio wavelengths (Türlér et al. 2000). This model derived from the model of Marscher & Gear (1985) describes analytically the evolution of synchrotron emission resulting from a shock wave moving down a relativistic jet. Compared to the model of van der Laan (1966) for an expanding plasma cloud it has the advantage to include the effects of both synchrotron and inverse-Compton energy losses.

Send offprint requests to: M. Türlér,
e-mail: Marc.Turler@obs.unige.ch

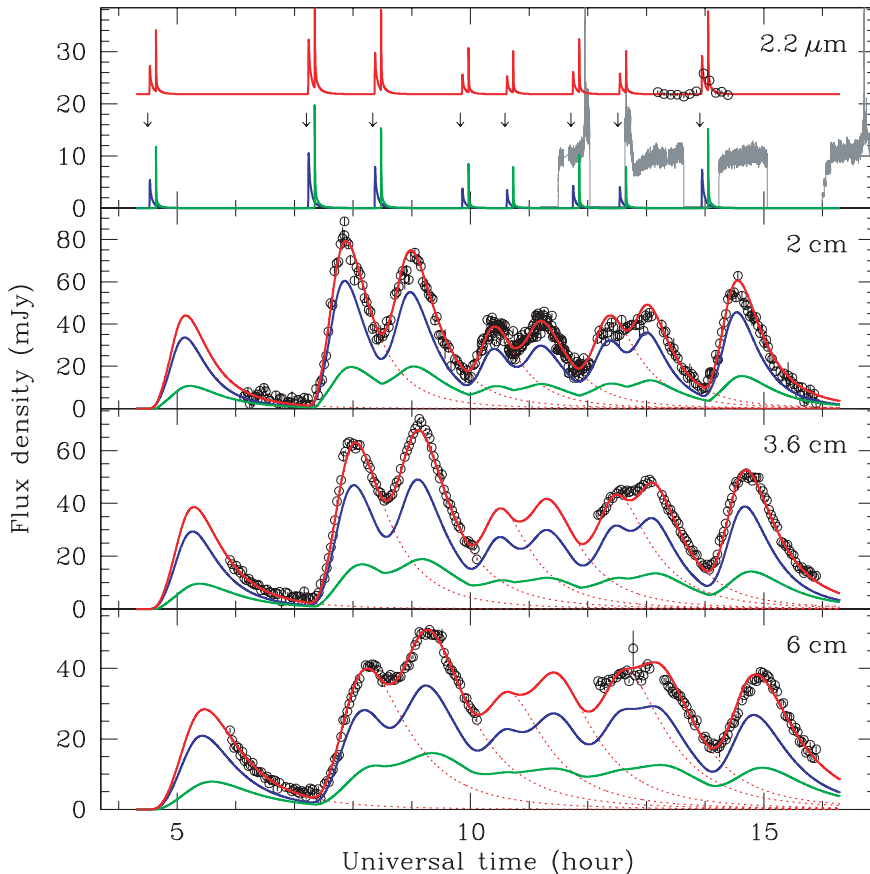


Fig. 1. Model fit to the infrared and radio observations of GRS 1915+105 on 15 May 1997. The points in the four panels show the time dependence of the emission at observed wavelengths of $2.2 \mu\text{m}$, 2 cm, 3.6 cm and 6 cm, from top to bottom. The $2.2 \mu\text{m}$ data are dereddened using a K -band absorption of 2.2 mag (Chapuis & Corbel 2004). The continuous red line is the best fit model, it is the sum of the emissions from the approaching jet (blue line) and the receding jet (green line) plus a constant flux at $2.2 \mu\text{m}$ fixed at 21.8 mJy. Red dotted lines separate the emission from distinct events. In the top panel, the onset times of the outbursts are indicated by arrows and the grey line is the X-ray light curve in the 2–60 keV band in units of 500 count s^{-1} .

2. Data and model

The data we use here are the radio oscillation events of GRS 1915+105 measured on 15 May 1997 (Mirabel et al. 1998; Dhawan et al. 2000). The Very Large Array (VLA) observations have the advantage to be very well sampled at three different radio wavelengths (see Fig. 1). The data start with a flux decrease followed by successive outbursts spaced by typically 1–2 h. These oscillation events are interpreted as ejections in a small jet that was observed simultaneously by the Very Long Baseline Array (VLBA) (see Dhawan et al. 2000, Fig. 9). Their evolution from short to long wavelengths is reminiscent of the observed behaviour of the bright quasar 3C 273 on a time scale of years (Türlér et al. 2000).

Additional data from the United Kingdom Infrared Telescope (UKIRT) in the $2.2 \mu\text{m}$ infrared band show a flux enhancement which is very likely the synchrotron precursor of the last radio outburst (Mirabel et al. 1998). The simultaneous X-ray measurements by the Rossi X-ray Timing Explorer (RXTE) in the 2–60 keV band present two flares apparently associated with two consecutive radio outbursts. This X-ray behaviour is indeed quite different from the light curve observed on 9 September 1997 which displays very rapid oscillations followed by a clear X-ray dip (Mirabel et al. 1998). A possible interpretation of this difference is that the X-ray flares of 15 May 1997 are not emitted by the accretion disc, but arise in the jet because of inverse-Compton scattering of synchrotron photons.

The Marscher & Gear (1985) shock model assumes a steady relativistic jet flow that can be disturbed by any increase of the pressure of the jet plasma or of its bulk velocity. If this disturbance is related to the accretion disc, it is likely to be symmetric in both jets. Starting as a sound wave, the disturbance will become supersonic at some point because of the decreasing pressure along the jet. The resulting shock wave will propagate down the jet and accelerate particles crossing the shock front. Accelerated electrons will then emit synchrotron radiation in the increased magnetic field of the compressed plasma behind the shock front. The evolution of the emitted spectrum depends on the dominant energy loss mechanism of the electrons. Just after the onset of the shock, inverse-Compton radiation is likely to be dominant, then synchrotron losses should become more important and finally adiabatic expansion, due to the widening of the jet, will dominate the energy losses. As a consequence, the turnover of the self-absorbed synchrotron spectrum will move from high to low frequencies following a characteristic three-stage path (see Fig. 2).

3. Method

To apply the model outlined above to the observed variability of GRS 1915+105 we use a methodology similar to the one used previously for 3C 273 (Türlér et al. 2000). There are however several modifications mainly implied by the specificity of GRS 1915+105, but including also some more general improvements. An important difference between the modelling of 3C 273 and GRS 1915+105 is that for the latter the emission

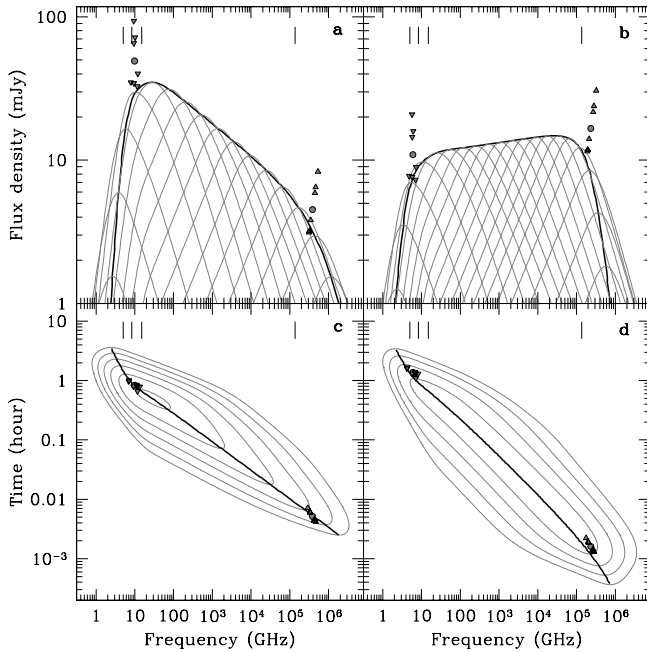


Fig. 2. Evolution of the synchrotron emission of an average model outburst in GRS 1915+105 on 15 May 1997. The observed evolution is different for the approaching jet (**a**, **c**) and the receding jet (**b**, **d**). The grey lines are synchrotron spectra at times spaced by 0.2 dex in **a**, **b**, and equal flux density contours spaced by 0.3 dex in **c**, **d**. The thick black line is the path followed by the turnover of the spectrum. The triangles show the position of the two stage transitions for each outburst as compared to their average position (circles). The frequency of the four light curves in Fig. 1 are indicated by vertical lines.

from the receding jet is well observed (Mirabel & Rodríguez 1994; Fender et al. 1999; Rodríguez & Mirabel 1999) and thus cannot be neglected. We take this into account by modelling each outburst as being the sum of twin outbursts, one arising in the approaching jet and the other in the receding jet. The observed emission from the two opposite jets is however different due to orientation and relativistic effects. We model this by two parameters, one being the ratio between the Doppler factors of the emitting material in the two jets and the second being the observed delay between the onset of the twin outbursts. In addition, the angle of 66° between the jet axis and the line of sight (Fender et al. 1999) is such that the shock is likely to be viewed sideways for the approaching jet and from behind for the receding jet (Marscher et al. 1992). This was taken into account in the modelling and results in a different observed evolution of the two jets (see Fig. 2).

To define the specificity of each outburst, we allow to vary from one event to the other only two out of the three parameters we used for 3C 273 (Türlér et al. 2000). These two parameters are the normalization K_{on} of the electron energy distribution ($N(E) = K E^{-s}$) and the magnetic field strength B_{on} at the onset of the shock. The bulk Doppler factor \mathcal{D}_{on} of the emitting material is assumed here to remain constant. Another simplification is that there does not seem to be a constant radio emission component in GRS 1915+105 similar to the hot spot at the far end of 3C 273's jet. Furthermore, the start of the radio light

curves of GRS 1915+105 can be simply modelled by the final decay of an outburst with average properties.

To have a more realistic model we replaced by progressive transitions the low- and high-frequency breaks of the synchrotron spectrum (see Türlér et al. 2000, Fig. 2) and we smoothed out the sharp edges of the three-stage evolution. The normalization of the synchrotron spectrum was redefined as the extrapolation of the optically thin slope, as in the original Marscher & Gear (1985) model. Finally, we introduced a new parameter to allow the frequency ratio ν_h/ν_m of the low frequency break to the turnover of the spectrum to vary with time. This allows to describe a synchrotron source which is first inhomogeneous and becomes progressively homogeneous near the transition to the final adiabatic expansion stage, as it seems to be the case in GRS 1915+105 (see Figs. 2a,b).

The model presented here has a total of 34 free parameters. 13 parameters are used to describe completely the shape and the evolution of the synchrotron spectrum for an average outburst in the approaching and the receding jets. The remaining 21 parameters are used to define the start times and the specificity of each distinct event. This model is the simplest jet model reproducing well the observations. It assumes a constant Doppler factor along the jet and a linear decrease $B \propto R^{-1}$ of the magnetic field B with the jet half-width R , as expected if B is perpendicular to the jet axis (Begelman et al. 1984). The model parameters are constrained by a simultaneous least-square fit to the 795 radio and infrared measurements of Fig. 1. This is achieved by many iterative fits of small subsets of the 34 parameters. The overall fit is shown in Fig. 1. Although the adjustment is not perfect (reduced χ^2 of 6.4), the shape of the light curves is very well reproduced by the model.

4. Results and discussion

The overall evolution of an average outburst in GRS 1915+105 as derived from the observations of 15 May 1997 is shown in Figs. 2a,c for the approaching jet and in Figs. 2b,d for the receding jet. The outburst is assumed to be intrinsically the same in both jets, but the observed evolution is different because of orientation effects. The different viewing angle changes the normalization, as well as the slopes of the three-stage evolution. The first effect is due to a different relativistic Doppler factor, while the second is due to the assumption that the approaching shock wave is viewed sideways, while the receding one is viewed from behind.

The model parameters describing the jet properties suggest that the jet when observed was rather dissipative and this could explain why it did not propagate very far (Dhawan et al. 2000). A first indication for this is the non-linear increase of the radius $R \propto L^r$ of the jet opening with distance L along the jet. The best fit value of $r = 1.52$ accounts for the rapid change of the spectral turnover frequency with time (see Figs. 2c,d). It suggests that the inner jet of GRS 1915+105 is more like a trumpet than a cone. This shape could result from a pressure gradient of the material surrounding the jet or from diverging external magnetic field lines channeling the jet plasma. Alternatively, it might be the signature of a decelerating jet flow. To test this hypothesis, we relax the constraint of a constant Doppler factor

along the jet. This results in a model with a slight tendency towards deceleration, but the improvement of the fit is not significant due to the lack of further infrared or submillimeter observations. There are however other indications suggesting a dissipative jet flow. In particular the fact that the obtained value of $s = 2.02$ for the index of the electron energy distribution $N(E) = K E^{-s}$ is close to 2. This means that there is roughly as much total energy carried by high-energy electrons than by low-energy electrons. For $s < 2$, the strong radiative losses of the dominant high-energy electrons would lead to a substantial pressure decrease along the jet and prevent the shock to propagate far (Marscher & Gear 1985). That such radiative losses are not negligible is also suggested by the slightly steeper decrease ($k = 3.10$) of the normalization $K \propto R^{-k}$ of the electron energy distribution than expected if the jet flow was really adiabatic ($k = 2(s + 2)/3 = 2.68$).

From the ratio of the relativistic Doppler factors in the receding and the approaching jet, we can derive the bulk speed of the emitting region. We obtain a ratio of 0.61, which corresponds, by assuming an angle of 66° between the jet axis and the line of sight (Fender et al. 1999), to a speed of $0.60c$, c being the speed of light. This mildly relativistic value contrasts with the speeds exceeding $0.9c$ derived for the giant eruptions (Fender et al. 1999; Rodríguez & Mirabel 1999), but is compatible with the hypothesis of a shock viewed sideways in the approaching jet provided that the jet opening half-angle is of 13° at least (Marscher et al. 1992). We can also estimate the distance from the black hole at which the shock wave forms based on the time interval between the onset of the outburst in the two jets. This interval is found to be ~ 400 s and corresponds to a distance from the black hole measured along the jet of 1.47×10^{13} cm, by assuming the same orientation as above. This is roughly 1 AU and is only about twice the separation of the binary system (Greiner et al. 2001).

Concerning the specificity of individual events, represented by the points in Fig. 2, we note that they do mostly differ in intensity from the average outburst. According to the model, this is due to changes of the normalization K_{on} of the electron energy distribution at the onset of the shock. The effect of significant changes of the magnetic field strength B_{on} from one event to the other would lead to a clear scatter of the points along the frequency axis, which is not observed (see Figs. 2a,b). The fact that the specificity of individual outbursts is mainly due to differences in the normalization K_{on} of the electron energy distribution is to be expected if the outbursts are due to an increased injection rate at the base of the jet. This finding therefore supports the idea that the shock waves forming in the jet of GRS 1915+105 are the result of instabilities in the inner accretion disc.

It is difficult to assess whether a scaled-up version of the shock model presented here could apply to the giant eruptions of GRS 1915+105. Their radio light curve with its very fast rise compared to its slow decay (Dhawan et al. 2000) resembles the infrared model light curve for the approaching jet, but expanded about 1000 times in duration and 100 times in amplitude. The optically thin synchrotron spectrum observed in the radio during the decay of major eruptions has also roughly the

same slope than the infrared spectrum deduced here. This analogy suggests that giant eruptions could be qualitatively similar events than those studied here, but with physical conditions such that their emission is shifted by orders of magnitude towards lower frequencies, longer time scales and enhanced fluxes.

5. Conclusion

This work shows that the microquasar GRS 1915+105 has, at least during some epochs, a variability behaviour similar to the quasar 3C 273, which can be modelled by shock waves propagating in a relativistic jet. This analogy suggests that the physical nature of relativistic jets and their emission is not dependent on the mass of the black hole at the origin of the ejection. The study of jets in both quasars and microquasars is therefore complementary. While quasars are bright and their jet structure is relatively well resolved, microquasars have the advantage of shorter variability time scales and of a less relativistic flow allowing us to observe also their counter-jet emission. The ability shown here to constrain jet emission models by multi-wavelength observations opens new perspectives for studying relativistic jets in quasars, microquasars and tentatively even in gamma-ray bursts.

Acknowledgements. We thank V. Dhawan for kindly providing use the VLBA data. Y.F. acknowledges financial support from the CNES.

References

- Atoyan, A. M., & Aharonian, F. A. 1999, MNRAS, 302, 253
- Begelman, M. C., Blandford, R. D., & Rees, M. J. 1984, Rev. Mod. Phys., 56, 255
- Belloni, T., Mendez, M., King, A. R., van der Klis, M., & van Paradijs, J. 1997a, ApJ, 488, L109
- Belloni, T., Mendez, M., King, A. R., van der Klis, M., & van Paradijs, J. 1997b, ApJ, 479, L145
- Chapuis, C., & Corbel, S. 2004, A&A, 414, 659
- Collins, R. S., Kaiser, C. R., & Cox, S. J. 2003, MNRAS, 338, 331
- Dhawan, V., Mirabel, I. F., & Rodríguez, L. F. 2000, ApJ, 543, 373
- Eikenberry, S. S., Matthews, K., Morgan, E. H., Remillard, R. A., & Nelson, R. W. 1998, ApJ, 494, L61
- Fender, R. P., Garrington, S. T., McKay, D. J., et al. 1999, MNRAS, 304, 865
- Greiner, J., Cuby, J. G., & McCaughrean, M. J. 2001, Nature, 414, 522
- Kaiser, C. R., Sunyaev, R., & Spruit, H. C. 2000, A&A, 356, 975
- Klein-Wolt, M., Fender, R. P., Pooley, G. G., et al. 2002, MNRAS, 331, 745
- Marscher, A. P., & Gear, W. K. 1985, ApJ, 298, 114
- Marscher, A. P., Gear, W. K., & Travis, J. P. 1992, in Variability of Blazars, 85–101
- Marscher, A. P., Jorstad, S. G., Gómez, J., et al. 2002, Nature, 417, 625
- Mirabel, I. F., Dhawan, V., Chaty, S., et al. 1998, A&A, 330, L9
- Mirabel, I. F., & Rodríguez, L. F. 1994, Nature, 371, 46
- Mirabel, I. F., & Rodríguez, L. F. 1998, Nature, 392, 673
- Rodríguez, L. F., & Mirabel, I. F. 1999, ApJ, 511, 398
- Türlér, M., Courvoisier, T. J.-L., & Paltani, S. 2000, A&A, 361, 850
- van der Laan, H. 1966, Nature, 211, 1131